

Scaling of conductance through quantum dots with magnetic field

I. J. Hamad and C. Gazza

*Instituto de Física Rosario. Facultad de Ciencias Exactas Ingeniería y Agrimensura,
Universidad Nacional de Rosario. Bv. 27 de Febrero 210 bis, 2000 Rosario, Argentina*

J. A. Andrade, A. A. Aligia, and P. S. Cornaglia

*Centro Atómico Bariloche and Instituto Balseiro,
Comisión Nacional de Energía Atómica, 8400 Bariloche, Argentina**

P. Roura-Bas

Dpto de Física, Centro Atómico Constituyentes, Comisión Nacional de Energía Atómica, Buenos Aires, Argentina

Using different techniques, and Fermi-liquid relationships, we calculate the variation with applied magnetic field (up to second order) of the zero-temperature equilibrium conductance through a quantum dot described by the impurity Anderson model. We focus on the strong-coupling limit $U \gg \Delta$ where U is the Coulomb repulsion and Δ is half the resonant-level width, and consider several values of the dot level energy E_d , ranging from the Kondo regime $\epsilon_F - E_d \gg \Delta$ to the intermediate-valence regime $\epsilon_F - E_d \sim \Delta$, where ϵ_F is the Fermi energy. We have mainly used density-matrix renormalization group (DMRG) and numerical renormalization group (NRG) combined with renormalized perturbation theory (RPT). Results for the dot occupancy and magnetic susceptibility from DMRG and NRG+RPT are compared with the corresponding Bethe ansatz results for $U \rightarrow \infty$, showing an excellent agreement once E_d is renormalized by a constant Haldane shift. For $U < 3\Delta$ a simple perturbative approach in U agrees very well with the other methods. The conductance decreases with applied magnetic field for dot occupancies $n_d \sim 1$ and increases for $n_d \sim 0.5$ or $n_d \sim 1.5$ regardless of the value of U . We also relate the energy scale for the magnetic-field dependence of the conductance with the width of low energy peak in the spectral density of the dot.

PACS numbers: 75.20.Hr, 71.27.+a, 72.15.Qm, 73.63.Kv

I. INTRODUCTION

In the last years an enormous amount of research in the field of nanoscience has been devoted to the transport through semiconducting¹⁻⁷ and molecular⁸⁻¹⁷ quantum dots (QDs), and to manifestations of the Kondo effect in these systems. The semiconducting QDs are artificial atoms created in two-dimensional electron gases by a suitable application of electrostatic voltages and are characterized by a high tunability of the parameters. By contrast in the molecular QDs, the molecule itself can be changed.

Many of these systems are described by the Anderson model for a magnetic impurity with spin 1/2 [Eq. 1 below], with constant hybridization V between the impurity level and the conduction electrons, whose unperturbed density of states ρ , can also be assumed constant. The main parameters of this model can be taken as the energy E_d of the level localized in the QD relative to the Fermi energy, which we take as $\epsilon_F = 0$, half the resonant level width $\Delta = \pi\rho V^2$ (in the literature sometimes the total width $\Gamma = 2\Delta$ is used), and the Coulomb repulsion U . As we shall see, the conduction electron band width $2D$ also plays a role, although a minor one. In the Kondo regime, $-E_d \gg \Delta$ and $E_d + U \gg \Delta$, all quantities depend on a single energy scale $T_K \sim D\sqrt{\rho J} \exp[-1/(\rho J)]$ with $J = 2V^2U/[-E_d(E_d + U)]$,¹⁸ and the localized spin at the QD is compensated by the conduction electrons result-

ing in a singlet ground state and maximum conductance (unitary limit) at temperatures $T \ll T_K$.^{4,6}

Recent experiments have studied the scaling laws for the conductance through one QD in the Kondo regime for small ($\ll T_K$) bias voltage V_b , temperature T and applied magnetic field.^{5,6,14} This stimulated further theoretical work on the subject concentrated mainly on the effect of a finite (although small) bias voltage, which is a tough non-equilibrium problem.¹⁹⁻²⁷ While it would be desirable to express the non-equilibrium properties in terms of thermodynamic ones, this task seems possible only for a limited number of coefficients in the expansion of the conductance.²⁴ Instead, at $T = 0$ and at equilibrium ($V_b = 0$), the magnetic-field dependence of the conductance, characterized by a coefficient c_B which was addressed theoretically recently,²⁸⁻³⁰ can be expressed in terms of the magnetic susceptibility and the second derivative of the dot occupancy with respect to the magnetic field,²⁹ using an extension of the Friedel sum rule³¹ to finite magnetic field for a spin conserving impurity model,^{32,33} used before in magnetotransport through quantum dots.³⁴⁻³⁶

The effects of magnetic field in systems of one and several QDs have been studied before experimentally^{1,37-41} and theoretically^{34,35,42-50} using several methods. The coefficient c_B has been calculated using numerical renormalization group (NRG) and a “superperturbation” approach^{25,27} recently.^{28,30} Unfortunately, the results

presented in Ref. 28, while exact at the symmetric point, are in general inaccurate because they miss a term proportional to the second derivative of the occupancy with respect to the magnetic field²⁹ (the effect of this term is responsible for the difference between top and middle lines in Fig. 1 below). Correct results were later presented,³⁰ but only in the weak coupling regime $U \leq 3\Delta$. For $U \rightarrow \infty$, the coefficient c_B was calculated using a slave-boson mean-field approximation (SBMFA).²⁹ However, direct comparison with NRG results shows that the SBMFA does not provide a reliable dot occupancy n_d ,⁵¹ and since n_d and its second derivative with respect to the magnetic field enter the expression of c_B [see Eq. (6)], the results of Ref. 29 are only qualitatively valid.

On the other hand, for $U \leq 3\Delta$, the possibility to reach the Kondo regime ($-E_d \gg \Delta$ and $E_d + U \gg \Delta$) is questionable and limited in any case to the symmetric situation $E_d = -U/2$. In general, in the Kondo regime, the spectral density presents two charge-transfer peaks at E_d and $E_d + U$ of total width 4Δ and a Kondo peak at the Fermi energy of total width $\sim 2T_K$.⁵²⁻⁵⁴ In the symmetric case $E_d = -U/2$ only one peak (at the Fermi level) is present for $U \leq 3\Delta$,⁵⁵ and as we shall discuss in this work, its half width at half maximum for $U = 3\Delta$ is 0.54Δ . The similarity of all energy scales and in particular the large T_K implies that one has to reach magnetic-field energies $g\mu_B B$ of the order of U to obtain a splitting in the spectral density *twice* $g\mu_B B$,³⁵ which is a distinctive signature of Kondo physics.^{42-45,59} For smaller magnetic fields the splitting is smaller. A splitting roughly consistent with $2g\mu_B B$ was observed in nonequilibrium transport through QDs.^{1,37-39} More recent experiments obtain a somewhat larger splitting. This is probably due to the fact that these experiments should not be interpreted in terms of the equilibrium spectral density and non-equilibrium calculations are necessary.^{35,46-48} In any case, to detect clearly the splitting one needs devices for which $T_K \ll U$.

Experimentally in semiconductor QDs a wide range of values of U/Δ are possible. Typical values of U are around 1-2 meV,^{1,5,7} and Δ can vary between 10 to 200 μeV , leading to ratios U/Δ near 10 in the first experiments,¹ 2 and 4.5 in the two devices studied by Kretinin *et al.*⁶, and larger than 50 in a recent system of two QDs.⁷ In contrast in molecular QDs the expected order of magnitude of U is ~ 1 eV for small molecules^{13,16} or ~ 0.1 eV for large molecules,⁹ while typical values of Δ are of the order of ~ 1 meV.^{13,16} Thus, the ratio U/Δ is several orders of magnitude and in practice one can take $U \rightarrow \infty$. These facts indicate the need to extend the reliable calculations of c_B (so far limited to the weak coupling regime $U \leq 3\Delta$) to more realistic values.

In addition, the molecular QDs are characterized by a high asymmetry of the coupling of the QD to the leads, and as a consequence, the shape of the differential conductance $G = dI/dV_b$ near zero applied bias voltage V_b reproduces the spectral density of the Kondo peak.^{54,60}

This renders possible to relate the energy scale of c_B with the width of the measured zero-bias anomaly as we shall discuss.

In this work we calculate c_B as a function of E_d for several values of U and in particular in the strong-coupling limit $U \rightarrow \infty$. We also calculate the half width at half maximum Δ_ρ of the low-energy peak in the spectral density of the dot for several values of E_d and U . As E_d increases from the symmetric case $E_d = -U/2$, c_B decreases, changes sign in the intermediate-valence regime $E_d \sim 0$ (where the occupancy $n_d \sim 0.6$) and becomes large and negative in the empty-orbital regime $E_d > 0$. As a function of n_d , c_B looks qualitatively similar for all values of U .

The paper is organized as follows. In Section II we present the model and equations that relate c_B with thermodynamic quantities. In Section III we describe briefly the different methods used. Section IV contains the results and Section V is a summary.

II. MODEL AND FORMALISM

The model is an Anderson impurity one in which a single localized level in a QD is hybridized with two conducting leads,

$$H = \sum_{\nu k \sigma} \epsilon_{\nu k} c_{\nu k \sigma}^\dagger c_{\nu k \sigma} + \sum_{\sigma} E_d n_{d\sigma} + U n_{d\uparrow} n_{d\downarrow} + \sum_{\nu k \sigma} (V_{\nu k} d_{\sigma}^\dagger c_{k\sigma} + \text{H.c.}) - g\mu_B B s_z, \quad (1)$$

where $c_{\nu k \sigma}^\dagger$ creates a conduction electron at the lead ν with momentum k and spin σ in the conduction band, d_{σ}^\dagger creates an electron in a localized level of the QD, $n_{d\sigma} = d_{\sigma}^\dagger d_{\sigma}$, and $s_z = (n_{d\uparrow} - n_{d\downarrow})/2$. By considering appropriate linear combinations of the electrons of both leads, the model is mapped into a single-channel model with resonant-level half-width at half-maximum $\Delta = \pi \sum_{\nu k} |V_{\nu k}|^2 \delta(\omega - \epsilon_k)$, which we assume independent of energy ω .

At zero temperature ($T = 0$) and at equilibrium (bias voltage $V_b = 0$), the contribution to the conductance of each spin for a given magnetic field $G_{\sigma}(B)$ is proportional to the corresponding density of states of the dot level $\rho_{d\sigma}(\omega, B)$ at the Fermi energy $\omega = 0$.^{54,61} In turn, this quantity is related to the occupancy for the corresponding spin by the Friedel sum rule³¹ generalized to finite B ³²⁻³⁴

$$\rho_{d\sigma}(0, B) = \frac{\sin^2(\pi n_{d\sigma})}{\pi \Delta}, \quad (2)$$

where for simplicity we denote as $n_{d\sigma}$ the expectation value of the corresponding operator. This allows to express the change of conductance by an applied magnetic field in terms of the occupancies

$$\frac{G(B)}{G(0)} = \frac{\rho_{d\uparrow}(0, B) + \rho_{d\downarrow}(0, B)}{\rho_{d\uparrow}(0, 0) + \rho_{d\downarrow}(0, 0)}. \quad (3)$$

Expanding $n_{d\sigma}$ up to second order in B one has²⁹

$$n_{d\sigma}(B) = \frac{n_d}{2} + \frac{\chi B}{g\mu_B}\sigma + \frac{\partial^2 n_d}{\partial B^2} \frac{B^2}{4} + O(B^3), \quad (4)$$

where $n_d = n_{d\uparrow} + n_{d\downarrow}$, χ is the magnetic susceptibility, $\sigma = 1$ (-1) for spin up (down) and the quantities in the second member except B are evaluated at $B = 0$.

From these equations, and defining c_B and T_0 (an energy scale of the order of T_K) by²⁸⁻³⁰

$$\begin{aligned} \frac{G(B)}{G(0)} &= 1 - c_B \left(\frac{g\mu_B B}{T_0} \right)^2, \\ \chi &= \frac{(g\mu_B)^2}{4T_0}, \end{aligned} \quad (5)$$

one obtains

$$\begin{aligned} c_B &= \frac{\pi^2}{16}(1 - c^2) - c \frac{\pi}{2} \left(\frac{T_0}{g\mu_B} \right)^2 \frac{\partial^2 n_d}{\partial B^2}, \\ \text{with } c &= \cot \left(\frac{\pi n_d}{2} \right). \end{aligned} \quad (6)$$

III. METHODS

As explained in the previous section, the calculation of the coefficient c_B that describes the magnetic-field dependence of the conductance at equilibrium and zero temperature, reduces to the calculation of the dot occupancy n_d , the magnetic susceptibility χ and the second derivative of the occupancy with magnetic field $\partial^2 n_d / \partial B^2$. We have used four methods to calculate these quantities.

A. Density-matrix renormalization group

We used density-matrix renormalization group (DMRG)⁶² to solve the impurity Anderson model for $U/\Delta = 3, 8$ and also for the infinite U case. The band was discretized using a Wilson chain¹⁸, with a discretization parameter Λ . This presents benefits that have already been introduced in the literature.⁶³⁻⁶⁵ In the range of parameters considered, the results do not change significantly when increasing the number of sites N beyond a certain value $N^*(\Lambda)$, as we have numerically verified for several values of Λ . We found that setting $\Lambda = 4$, $N = 50$, and retaining $m = 600$ states was enough to assure convergence, being the truncation error (the weight of the neglected states in the density matrix) 10^{-6} in the worst case, reassuring the reliability of the calculation. The DMRG results in this paper correspond to these values of Λ , N and m .

As a consequence of this discretization, the density of conduction states at the Fermi level $\rho_\Lambda(0)$ decreases with

respect to the continuum limit $\Lambda \rightarrow 1$. We have calculated $\rho_\Lambda(0)$ numerically for the Wilson chain without dot, and determined the hybridization V_Λ of the dot with the first site of the chain from the condition $\pi\rho_\Lambda(0)V_\Lambda^2 = \Delta$.

We have chosen a half band width $D = 100\Delta$ since the ratio D/Δ is very large in real systems.

We have calculated the ground state energy and the occupancy of the impurity for different values of the magnetic field B , which was applied to the impurity site only, as in Eq. (1). For the calculation of the susceptibility and $\partial^2 n_d / \partial B^2$, the general criterion used was to calculate the ground-state energy and magnetization at the dot for ten different values of the magnetic field B such that $B_{min} < B < B_{max}$, where $g\mu_B B_{min} = 0.005T_K^0$, and $B_{max} \approx 150B_{min}$. The curves were smooth and very well approximated by linear or quadratic polynomials, depending on the case. The susceptibility was calculated both as the derivative of the magnetization of the dot with respect to B fitting the curve with a straight line through the origin, and as the second derivative of the ground state energy with respect to B fitting with a quartic polynomial and extracting the coefficient of the quadratic term. In all cases the agreement was complete.

B. Numerical renormalization group plus renormalized perturbation theory

We have used the standard Numerical renormalization group (NRG)^{66,67} to calculate the occupancy n_d and its second derivative with respect to the magnetic field $\partial^2 n_d / \partial B^2$. The latter was obtained calculating n_d for nearly 10 different magnetic fields in the interval $0 < g\mu_B B < \tilde{\Delta}$, where $\tilde{\Delta}$ is defined below and fitting the points with a B^2 dependence.

We used a discretization parameter $\Lambda = 3.5$ and truncated the spectrum, after the fifth iteration, keeping up to 2000 states. In contrast to the DMRG calculations, we take $D = 10\Delta$ and do the numerical calculations using a hybridization $V_\Lambda = \sqrt{A_\Lambda}V$ between the dot and the first conduction site in the Wilson chain, where $\Delta = \pi V^2 / (2D)$ and

$$A_\Lambda = \frac{\Lambda + 1}{2\Lambda - 2} \ln \Lambda. \quad (7)$$

This expression has been suggested to obtain the correct Kondo temperature in the Kondo limit.^{66,68}

For the magnetic susceptibility χ one has the problem that in the Kondo regime (large U and $\Delta \ll |E_d|, E_d + U$) it oscillates as the iterations increase (lowering the temperature). One way to solve this problem is to use $\Lambda \gg 1$ and average over several realizations of the logarithmic grid,⁶⁹ but we obtained only a moderate improvement. A better method is to use the full density matrix within the NRG, although still in the strong coupling limit, values of the Wilson ratio R above 2 and about 3% larger than the exact ones were obtained.⁶⁹ Here we have obtained

renormalized parameters \tilde{E}_d , $\tilde{\Delta}$ and \tilde{U} that describe the low-energy physics, following the procedure explained by Hewson *et al.* in Ref. 70. The only difference is that we interpret that in Eq. (42) of that paper, the first member refers to $\tilde{\Delta}_\Lambda$ the renormalized Δ for $\Lambda \neq 1$, which is related to $\tilde{\Delta}$ by $\tilde{\Delta}_\Lambda = A_\Lambda \tilde{\Delta}$. From the renormalized parameters, the susceptibility is obtained accurately using renormalized perturbation theory (RPT) to second order in $\tilde{U}/(\pi\tilde{\Delta})$.³³ The result is

$$\chi = (g\mu_B)^2 \tilde{\rho}_d(0) R/2, \quad (8)$$

where the Wilson ratio and the quasiparticle spectral density at the dot are

$$R = 1 + \tilde{U} \tilde{\rho}_d(0), \quad (9)$$

$$\tilde{\rho}_d(\omega) = \frac{\tilde{\Delta}/\pi}{(\omega - \tilde{E}_d)^2 + \tilde{\Delta}^2}. \quad (10)$$

Using this procedure we obtain for example for $U = 10\Delta$ and $E_d = -U/2$, a Wilson ratio $R = 1.9939$, while the exact result from Bethe ansatz (see Section III C) is 1.9957 and NRG with the full density matrix gives 2.024.⁶⁹

The quasiparticle spectral density is modified by the renormalized interaction \tilde{U} .³³ To calculate the width of the resulting renormalized spectral density we use ordinary perturbation theory (PT)^{56,57} to second order in $\tilde{U}/(\pi\tilde{\Delta})$, taking \tilde{E}_d as the effective dot energy. Since even for $U \rightarrow \infty$, $\tilde{U}/(\pi\tilde{\Delta})$ is of the order of 1 (see Table II), the second order results are accurate enough. To illustrate the consistency of the procedure, if one uses directly PT for $U = 3\Delta$ in the symmetric case $E_d = -U/2$, one obtains a half width at half maximum Δ_ρ of the low-energy peak in the spectral density of the dot, only about 2% higher ($\Delta_\rho = 0.558\Delta$) than the result $\Delta_\rho = 0.545\Delta$ that comes determining first the renormalized parameters by NRG and then using PT. As T_0 , Δ_ρ is also of the order of the Kondo temperature T_K in units for which the Boltzmann constant $k_B = 1$.

C. Bethe ansatz

As a check to the results obtained with the methods described above, we have calculated the occupancy and magnetic susceptibility for $U \rightarrow \infty$ and several values of a shifted dot energy E_d^* at $T = 0$ using integral analytical expressions obtained with the Bethe ansatz in Ref. 71 and as a particular case of a more general model in Ref. 72. Some tricks to deal with singularities in the integrals were used, which are explained in the appendix of Ref. 73. Unfortunately, to obtain an analytical exact expression for the second derivative of the occupancy with magnetic field $\partial^2 n_d / \partial B^2$, is very difficult and is beyond

the scope of the present paper. This precludes to give exact results for c_B out of the symmetric case $E_d = -U/2$.

In the symmetric case, V. Zlatić and B. Horvatić have shown that the exact results for the magnetic susceptibility and quasiparticle weight $z = \tilde{\Delta}/\Delta$ can be expressed as a convergent power series.⁷⁴ We have evaluated this series using a FORTRAN program in quadruple precision. From these results we have derived the renormalized parameters and the Wilson ratio for comparison.

D. Interpolative perturbative approximation

For small values of U/Δ one may use the interpolative perturbative approximation (IPA) which is a modification of the PT approach to second order in U/Δ modified to reproduce exactly the atomic limit $U/\Delta \rightarrow +\infty$.⁷⁵⁻⁷⁸ In addition, the on-site term is split as $\sum_\sigma E_d n_{d\sigma} = \sum_\sigma E_d^{\text{eff}} n_{d\sigma} + \sum_\sigma (E_d - E_d^{\text{eff}}) n_{d\sigma}$, where the second term is included in the perturbation, and E_d^{eff} is determined to optimize the results. In particular, in Ref. 78, E_d^{eff} was determined to satisfy the Friedel sum rule. Results for the conductance through a QD using the IPA⁷⁹ agree with more recent ones using the finite temperature density matrix renormalization group method.⁸⁰

Here we use the spin dependent version in which $E_{d\sigma}^{\text{eff}}$ depends on spin and is determined self-consistently for each spin to satisfy the corresponding Friedel sum rule Eq. (2).³⁵ Comparison with exact results without magnetic field shows that the IPA provides very accurate values for the occupancy n_d as a function of E_d for $U/\Delta \leq 6$. The maximum deviation is less than 1 % for $U/\Delta = 6$.⁷³

IV. RESULTS

In this section, we provide results of the coefficient c_B of the magnetic-field dependence of the conductance [see Eq. (5)] and the energy scale T_0 as a function on the energy level of the QD E_d which is easily controlled by a gate voltage in transport experiments. Since T_0 is determined by the magnetic susceptibility χ [see Eq. (5)] which is not accessible in transport experiments, we also provide a relation between T_0 and the half width at half maximum of the spectral density Δ_ρ . In experiments with high asymmetry in the coupling between the dot and both leads and in the Kondo regime, the differential conductance as a function of bias voltage $G(V_b) = dI/dV_b$ directly represents the Kondo peak in the spectral density.^{54,60} For less asymmetry and entering in the intermediate-valence regime, the half width at half maximum of the zero-bias peak in G times the electric charge e (Δ_G) increases to about 1.6 Δ_ρ but remains of the same order of magnitude for $U \rightarrow \infty$.⁵⁴

We focus our study in three values of U/Δ : 3, which is the largest value for which previous NRG results were reported,³⁰ $U \rightarrow \infty$ which corresponds to the molecular QDs, and an intermediate case $U/\Delta = 8$ which is a

reasonable value for semiconducting QDs in the Kondo regime.

A. $U/\Delta = 3$

In Fig. 1 we represent the coefficient of the magnetic-field dependence of the conductance [see Eq. (5)] as a function of the on-site energy for $U = 3\Delta$ and three different methods. Because of a particular electron-hole symmetry (see Section II.C.1 of Ref. 84), $c_B(E_d) = c_B(-U - E_d)$, or in other words, for $-U \leq E_d \leq -U/2$, c_B is the specular image around $E_d = -U/2$ of the results represented in Fig. 1. Our DMRG (NRG + RPT) results were obtained in intervals of $\Delta/4$ ($\Delta/2$) between the symmetric case $E_d = -U/2$ and $E_d = 0$. These results agree between them and also with the corrected NRG ones of Merker *et al.*³⁰ To compare with these results, we have digitalized the results of c'_B given in Fig. 1 of Ref. 30 and used the relation

$$\frac{c'_B}{c_B} = \left(\frac{T_0^{\text{sym}}}{T_0} \right)^2 = \left(\frac{\chi}{\chi^{\text{sym}}} \right)^2, \quad (11)$$

where the superscript “sym” refers to the symmetric case $E_d = -U/2$. There is a small discrepancy for $E_d = 0$, where the results of Merker *et al.* lie slightly above ours. This might be due to the fact that their results were calculated directly from the conductance, while ours use only thermodynamic quantities and are expected to be more accurate. In fact we have also calculated c_B from the conductance derived from the spectral density calculated with the full-density-matrix NRG for a few points, but the results showed some deviations from the results obtained with DMRG and NRG+RPT using Eq. (6).

We also show in Fig. 1 the result of c_B within DMRG including only the first term of c_B [neglecting the second negative term proportional to $\partial^2 n_d / \partial B^2$ in Eq. (6)] and compared with the corresponding result in Fig. 6 of Ref. 28. There is again a good agreement with the results of Ref. 30 indicating a coincidence (except for deviations imperceptible in the figure) between the corresponding results for the occupancy n_d in the range of E_d studied. Although not shown in the figure, the first term of c_B (which depends only on the occupancy n_d) within NRG+RPT and IPA also coincides with the results shown, because all these methods provide accurately values for n_d . Instead the full result requires the calculation of the magnetic susceptibility χ and $\partial^2 n_d / \partial B^2$ for which the IPA fails at large U as explained below.

The correction due to the second derivative of the occupancy becomes significant in the intermediate-valence regime, in particular at $E_d = 0$, where it leads to a change of sign in c_B [for all for all parameters considered in this paper, the first (second) term in Eq. (6) is positive (negative)]. The effect of this correction (or in

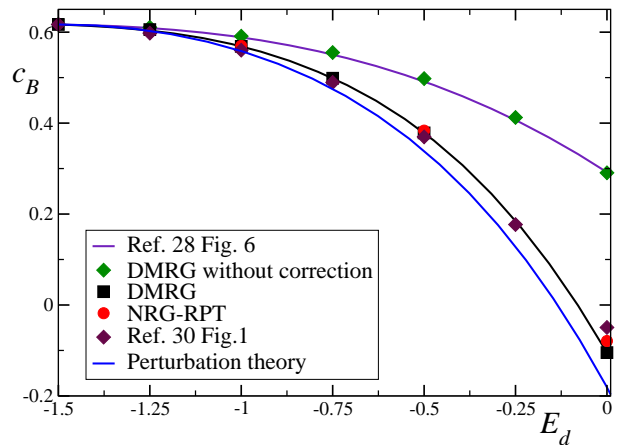


FIG. 1: (Color online) c_B vs E_d for $U = 3\Delta$ obtained by different methods.

general the difference between different approximations for c_B) is not so evident in the curve c'_B vs E_d because the magnetic susceptibility decreases strongly as E_d enters in the intermediate-valence regime (particularly for large U) and then the values of $|c'_B|$ are largely reduced with respect to c_B [by a factor 5.5 according to Eq. (11) for $E_d = 0$]. The different approaches lead to the exact result $c_B = c'_B = \pi^2/16 \approx 0.617$ in the symmetric case $E_d = -U/2$,^{28-30,81} and for large enough U the values of c'_B lie near zero for $E_d = 0$, even neglecting $\partial^2 n_d / \partial B^2$, because of the factor $(T_0^{\text{sym}}/T_0)^2$.

The values of c_B obtained using IPA lie slightly below those of the other methods (in c'_B vs E_d the maximum deviation is near 0.02). We have verified that the occupancy is very well reproduced by the IPA (with an underestimation of the order of 1 %) in agreement with a previous comparison with Bethe-ansatz results.⁷³ Therefore, the first term (positive in the range of E_d shown) of c_B in Eq. (6) is well reproduced. However, the remaining negative term is overestimated due to an underestimation of the magnetic susceptibility χ (overestimation of T_0) by 6% and an overestimation of $\partial^2 n_d / \partial B^2$ that reaches of the order of 10% for E_d near $-\Delta$. The accuracy of the IPA depends strongly on the perturbation parameter $U/(\pi\Delta)$. For example in the symmetric case $E_d = -U/2$, the IPA result for χ is below the Bethe ansatz results by 15% for $U = 4\Delta$ and by only 1.4% for $U = 2\Delta$.

One disadvantage of c_B with respect to c'_B is that the energy scale used as a reference, T_0 , depends on E_d [see Eq. (5)] and one needs to know two numbers for each E_d (c_B and T_0) to describe the magnetic-field dependence of the conductance. An advantage is that T_0 is of the order of the Kondo temperature, which in turn is proportional to the width $2\Delta_G/e$ of the zero-bias peak in the conductance (which is experimentally accessible) and to the width $2\Delta_\rho$ of the spectral density of the dot state. All these quantities are of the order of the quasiparticle level width $\tilde{\Delta}$. In Table I we give values obtained from RPT+NRG of these quantities, except Δ_G . This width

is addressed in Ref. 54 where it is shown that in the Kondo regime for strongly asymmetric leads (as usual in molecular QDs) $\Delta_G = \Delta_\rho$.⁶⁰

TABLE I: Effective parameters, half width of the spectral density Δ_ρ and ratio Δ_ρ/T_0 obtained from NRG+RPT for $U = 3\Delta$ and several values of E_d .

E_d/Δ	$\tilde{\Delta}/\Delta$	$\tilde{E}_d/\tilde{\Delta}$	$\tilde{U}/(\pi\tilde{\Delta})$	$\Delta_\rho/\tilde{\Delta}$	Δ_ρ/T_0
-1.5	0.639	0	0.738	0.835	0.944
-1	0.671	0.196	0.732	0.848	0.885
-0.5	0.754	0.421	0.716	0.883	0.766
0	0.845	0.700	0.698	0.930	0.581

The Bethe-ansatz result of $\tilde{\Delta}$ for $E_d = -1.5\Delta$ is 0.6522, slightly larger than the RPT+NRG tabulated. This is due to the fact that for this calculation we used a finite half band width $D = 10\Delta$ that affects the Kondo temperature. However the Wilson ratio 1.738 is almost the same as the exact one 1.741. The ratio Δ_ρ/T_0 evolves from near 1 in the symmetric case $E_d = -U/2$ to near 1/2 for $E_d = 0$. From the data given in Table I and Fermi-liquid relations one can obtain the occupancy

$$n_d = 1 - \frac{2}{\pi} \arctan\left(\frac{\tilde{E}_d}{\tilde{\Delta}}\right), \quad (12)$$

which coincides in general within 1 % with the corresponding result obtained directly with NRG.

B. $U \rightarrow \infty$

Experimentally, the on-site energy of the dot level E_d is controlled by the gate voltage and determined by capacitance effects of all applied gate voltages^{7,54,82,83} (see for example the supplementary material of Ref. 7). The position of the Coulomb blockade edges and the related charge-transfer peaks in the spectral density of the dot level are determined by a shifted energy E_d^* which contains the effects of a renormalization due to the hybridization with the leads.^{54,85} This shift is significant when both, the half band width D and the Coulomb repulsion U are much larger than Δ , as in many realistic systems. In particular for $U \rightarrow \infty$, the calculation by Haldane based on poor man's scaling gives

$$\delta = E_d^* - E_d = \frac{\Delta}{\pi} \ln\left(\frac{D}{\alpha\Delta}\right), \quad (13)$$

where $\alpha \sim 1$. Experimentally, E_d^* is accessible but not E_d . For example at temperatures above the Kondo temperature, a maximum in the equilibrium conductance takes place for $E_d^* = 0$, or for finite E_d^* Coulomb edges appear for bias voltages such that $V_b = \pm E_d^*/e$.⁵⁴

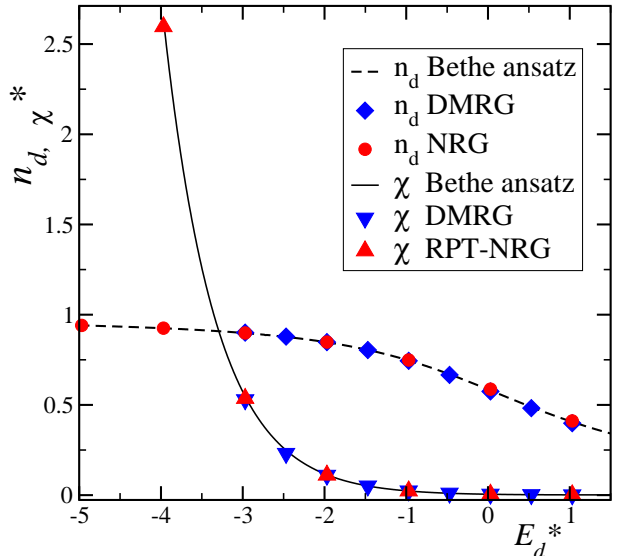


FIG. 2: (Color online) occupancy and scaled magnetic susceptibility $\chi^* = \chi\Delta/[100(g\mu_B)^2]$ for $U \rightarrow \infty$ as a function of the shifted dot energy for different techniques.

In order to compare the DMRG results for the occupancy n_d and magnetic susceptibility χ for fixed E_d with the corresponding analytical Bethe-ansatz (in which $D \rightarrow \infty$ is assumed) as a function of E_d^* , we have to determine the shift δ_{DMRG} . We obtain that *both* functions n_d and χ shifted by *the same* $\delta_{\text{DMRG}} = 1.53\Delta$ coincide with the corresponding Bethe-ansatz results, as shown in Fig. 2. This result is consistent with Eq. (13) which gives $\delta = 1.47\Delta$ for $D = 100\Delta$ and $\alpha = 1$. The same happens with the NRG+RPT results using $\delta_{\text{NRG}} = 1.00\Delta$. For large negative values of E_d/Δ the occupancy flattens near 1, and the susceptibility increases strongly due to the exponential dependence of the Kondo temperature T_K on E_d^* and the fact that χ is proportional to $1/T_K$ in the Kondo regime.

Once the shifts δ are determined, we can represent c_B as a function of E_d^* using both methods. The results are shown in Fig. 3. For $E_d^*/\Delta < -2$, as the occupancy $n_d > 0.84$ and the system is in the Kondo regime, $c_B > 0.5$ indicating a small to moderate deviation from the value $(\pi/4)^2 \approx 0.617$ of the symmetric case. In this region, the correction due to the second (negative) term of c_B in Eq. (6) is below 1 %. Instead, for $E_d^*/\Delta > -2$, c_B decreases rapidly and changes sign for $E_d^*/\Delta \approx 0$, in the middle of the intermediate-valence region.

In Table II we list the renormalized parameters and ratios of different quantities proportional to T_K obtained with NRG+RPT. As it is expected in the Kondo regime $-E_d \gg \Delta$ and $E_d + U \gg \Delta$, the Kondo temperature depends exponentially on E_d for $E_d/\Delta < -2$. However, in this regime, particularly for $E_d/\Delta = -3$, the ratios $\Delta_\rho/\tilde{\Delta}$ and Δ_ρ/T_0 are almost constant, near 0.7 and 0.85

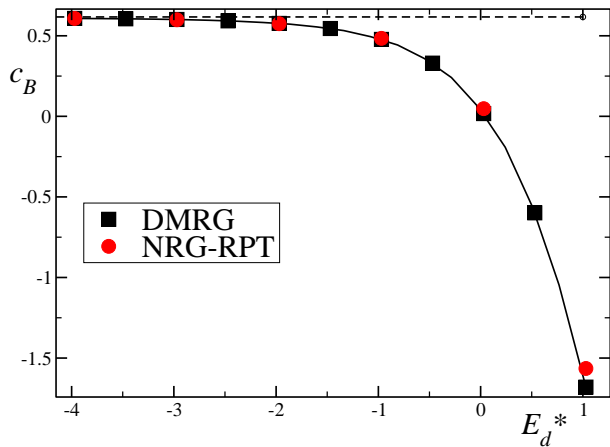


FIG. 3: (Color online) c_B vs E_d^* for $U \rightarrow \infty$ obtained by DMRG and NRG+RPT.

TABLE II: Effective parameters, half width of the spectral density Δ_ρ and ratio Δ_ρ/T_0 obtained from NRG+RPT for $U \rightarrow \infty$ and several values of E_d .

E_d/Δ	$\tilde{\Delta}/\Delta$	$\tilde{E}_d/\tilde{\Delta}$	$\tilde{U}/(\pi\tilde{\Delta})$	$\Delta_\rho/\tilde{\Delta}$	Δ_ρ/T_0
-6	2.51×10^{-4}	0.0937	1.009	0.706	0.892
-5	1.21×10^{-3}	0.118	1.014	0.705	0.886
-4	5.79×10^{-3}	0.160	1.025	0.703	0.873
-3	0.0270	0.243	1.054	0.699	0.838
-2	0.115	0.416	1.136	0.693	0.740
-1	0.356	0.766	1.317	0.716	0.530
0	0.640	1.338	1.594	0.793	0.286

respectively. Instead, entering the intermediate valence regime, $\Delta_\rho/\tilde{\Delta}$ slightly increases and Δ_ρ/T_0 strongly decreases.

C. $U/\Delta = 8$

In Fig. 4 we show the c_B for $U = 8\Delta$ obtained by DMRG and NRG+RPT. While the results of both methods coincide in the Kondo regime ($E_d \leq -2\Delta$ in the figure) there are some deviations in the intermediate valence regime. This is due to the fact that for finite U the Haldane shift δ depends on E_d , being 0 in the symmetric case $E_d = -U/2$, positive for $E_d > -U/2$ and larger for larger D . Therefore, the DMRG results calculated with D 10 times larger, correspond to larger E_d^* in general, but for both techniques $E_d^* = E_d$ in the symmetric case.

Table III displays the renormalized parameters and ratios $\Delta_\rho/\tilde{\Delta}$, Δ_ρ/T_0 obtained with NRG+RPT. As in the case $U \rightarrow \infty$, these ratios are nearly constant in the Kondo regime (although the variation is more pronounced as before) $-E_d \gg \Delta$ and $E_d + U \gg \Delta$, while

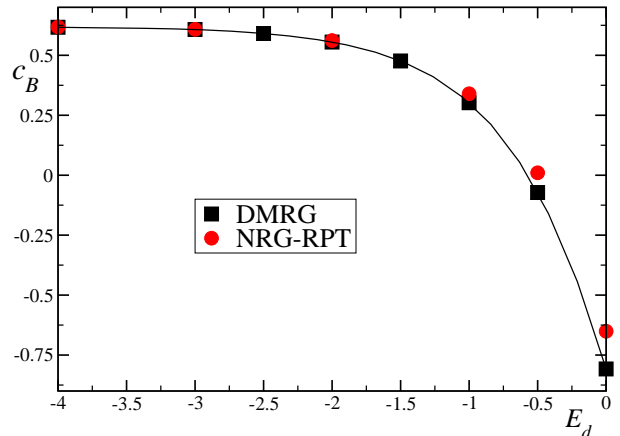


FIG. 4: (Color online) c_B vs E_d $U = 8\Delta$ obtained by DMRG and NRG+RPT.

TABLE III: Effective parameters, half width of the spectral density Δ_ρ and ratio Δ_ρ/T_0 obtained from NRG+RPT for $U = 8\Delta$ and several values of E_d .

E_d/Δ	$\tilde{\Delta}/\Delta$	$\tilde{E}_d/\tilde{\Delta}$	$\tilde{U}/(\pi\tilde{\Delta})$	$\Delta_\rho/\tilde{\Delta}$	Δ_ρ/T_0
-4	0.120	0	0.985	0.715	0.902
-3	0.143	0.101	0.987	0.718	0.895
-2	0.235	0.247	1.004	0.724	0.845
-1	0.457	0.510	1.040	0.759	0.699
-0.5	0.609	0.515	1.060	0.802	0.573
0	0.746	0.977	1.081	0.857	0.430

in the intermediate valence regime, $\Delta_\rho/\tilde{\Delta}$ increases and Δ_ρ/T_0 decreases markedly (although not so strongly as for $U \rightarrow \infty$). The Bethe ansatz result of $\tilde{\Delta}/\Delta = 0.1326$ for $E_d/\Delta = -4$ is about 10 % larger than the NRG+RPT result. As for $U = 3\Delta$ this difference is due to the effect of the finite band width $2D$ of the conduction band on the Kondo temperature, and practically does not alter the Wilson ratio.

D. c_B as a function of occupancy

In Fig. 5 we represent our main results of c_B as functions of the occupancy and the corresponding result for $U \rightarrow \infty$ obtained previously using slave bosons in the mean-field approximation (SBMFA).²⁹ We also include the results using the interpolative perturbative approximation (see Section III D) for $U = 2$. In spite of the very different values of U used, all curves look qualitatively similar. There is a slightly more pronounced decrease of c_B vs $1 - n_d$ for smaller values of U , c_B changes sign at $n_d \sim 0.64$ for $U = 2$ and at $n_d \sim 0.57$ for $U \rightarrow \infty$. Curiously, the SBMFA gives values that lie in between

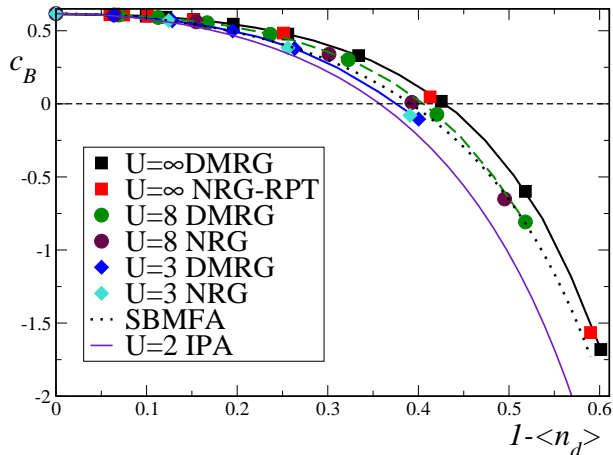


FIG. 5: (Color online) c_B vs $1 - n_d$ for different values of U obtained by DMRG and NRG+RPT, and for $U \rightarrow \infty$ using slave bosons in the mean-field approximation.

those for $U = 3\Delta$ and those for $U = 8\Delta$, although it is intended for $U \rightarrow \infty$.

V. SUMMARY

Using different techniques (mainly DMRG and NRG+RPT) we have calculated the coefficient of the magnetic-field dependence of the conductance [see Eq. (6)] for several values of U focusing on the strong-

coupling limit $U \gg T_K$. As it is known, $c_B = (\pi/4)^2$ in the symmetric case $E_d = -U/2$, where the occupancy $n_d = 1$. As E_d increases or decreases, c_B decreases and changes sign in the intermediate valence cases where $E_d^* \sim \epsilon_F$ or $E_d^* + U \sim \epsilon_F$, where E_d^* is a renormalized energy that includes the Haldane shift (which is important for large U) and ϵ_F is the Fermi energy. In these cases (related by a special electron-hole transformation) the occupancy n_d is near 0.6 or 1.4 respectively.

We have also provided quantitative results for the ratio of the energy scale of the magnetic-field dependence of the conductance and the magnetic susceptibility T_0 [see Eq. (6)] with the half width at half maximum of the spectral density Δ_ρ . For devices in which the coupling to the left and right leads are very different, this quantity coincides with the half width at half maximum Δ_G of the zero-bias peak in G times the electric charge e and is experimentally accessible.^{54,60} For more symmetric devices Δ_G/Δ_ρ increases and some values are tabulated in Ref. 54.

When c_B is represented as a function of the occupancy n_d for different values of U , the curves $c_B(n_d)$ look qualitatively similar.

Acknowledgments

We thank Luis O. Manuel for useful discussions. We are partially supported by CONICET, Argentina. This work was sponsored by PICT 2013-1045 of the ANPCyT-Argentina, PIP 112-201101-00832, PIP 112-201201-00389, PIP 112-201201-01060 and PIP 112-201201-00273 of CONICET.

* Electronic address: aligia@cab.cnea.gov.ar

¹ D. Goldhaber-Gordon, H. Shtrikman, D. Mahalu, D. Abusch-Magder, U. Meirav, and M. A. Kastner, *Nature* **391**, 156 (1998).

² S. M. Cronenwett, T. H. Oosterkamp, and L. P. Kouwenhoven, *Science* **281**, 540 (1998).

³ D. Goldhaber-Gordon, J. Göres, M. A. Kastner, H. Shtrikman, D. Mahalu, and U. Meirav, *Phys. Rev. Lett.* **81**, 5225 (1998).

⁴ W.G. van der Wiel, S. de Franceschi, T. Fujisawa, J.M. Elzerman, S. Tarucha, and L.P. Kouwenhoven, *Science* **289**, 2105 (2000).

⁵ M. Grobis, I. G. Rau, R. M. Potok, H. Shtrikman, and D. Goldhaber-Gordon, *Phys. Rev. Lett.* **100**, 246601 (2008).

⁶ A. V. Kretinin, H. Shtrikman, D. Goldhaber-Gordon, M. Hanl, A. Weichselbaum, J. von Delft, T. Costi, and D. Mahalu, *Phys. Rev. B* **84**, 245316 (2011).

⁷ S. Amasha, A. J. Keller, I. G. Rau, A. Carmi, J. A. Katine, H. Shtrikman, Y. Oreg, and D. Goldhaber-Gordon, *Phys. Rev. Lett.* **110**, 046604 (2013).

⁸ W. Liang, M. P. Shores, M. Bockrath, J. R. Long, and H. Park, *Nature* **417**, 725 (2002).

⁹ S. Kubatkin, A. Danilov, M. Hjort, J. Cornil, J. L. Brédas, N. Stuhr-Hansen, P. Hedegård, and Th. Bjørnholm, *Nature*

425, 699 (2003).

¹⁰ L. H. Yu, Z. K. Keane, J. W. Ciszek, L. Cheng, J. M. Tour, T. Baruah, M. R. Pederson, and D. Natelson, *Phys. Rev. Lett.* **95**, 256803 (2005).

¹¹ M. N. Leuenberger and E. R. Mucciolo, *Phys. Rev. Lett.* **97**, 126601 (2006).

¹² J. J. Parks, A. R. Champagne, G. R. Hutchison, S. Flores-Torres, H. D. Abruña, and D. C. Ralph, *Phys. Rev. Lett.* **99**, 026601 (2007).

¹³ N. Roch, S. Florens, V. Bouchiat, W. Wernsdorfer, and F. Balestro, *Nature* **453**, 633 (2008).

¹⁴ G. D. Scott, Z. K. Keane, J. W. Ciszek, J. M. Tour, and D. Natelson, *Phys. Rev. B* **79**, 165413 (2009).

¹⁵ J. J. Parks, A. R. Champagne, T. A. Costi, W. W. Shum, A. N. Pasupathy, E. Neuscamman, S. Flores-Torres, P. S. Cornaglia, A. A. Aligia, C. A. Balseiro, G. K.-L. Chan, H. D. Abruña, and D. C. Ralph, *Science* **328**, 1370 (2010).

¹⁶ S. Florens, A. Freyn, N. Roch, W. Wernsdorfer, F. Balestro, P. Roura-Bas and A. A. Aligia, *J. Phys. Condens. Matter* **23**, 243202 (2011).

¹⁷ R. Vincent, S. Klyatskaya, M. Ruben, W. Wernsdorfer, and F. Balestro, *Nature (London)* **488**, 357 (2012).

¹⁸ K. G. Wilson, *Rev. Mod. Phys.* **47**, 773 (1975).

¹⁹ J. Rincón, A. A. Aligia, and K. Hallberg, *Phys. Rev. B* **79**,

- 121301(R) (2009); arXiv:0901.4326.
- ²⁰ E. Sela and J. Malecki, Phys. Rev. B **80**, 233103 (2009).
- ²¹ Z. Ratiani and A. Mitra, Phys. Rev. B **79**, 245111 (2009).
- ²² P. Roura-Bas, Phys. Rev. B **81**, 155327 (2010).
- ²³ C. A. Balseiro, G. Usaj, and M. J. Sánchez, J. Phys. Condens. Matter **22**, 425602 (2010).
- ²⁴ A. A. Aligia, J. Phys. Condens. Matter **24**, 015306 (2012).
- ²⁵ E. Muñoz, C. J. Bolech, and S. Kirchner, Phys. Rev. Lett. **110**, 016601 (2013); *ibid* **111**, 089702 (2013); A. A. Aligia, Phys. Rev. Lett. **111**, 089701 (2013); A. A. Aligia, arXiv:1310.8324.
- ²⁶ A. A. Aligia, Phys. Rev. B **89**, 125405 (2014).
- ²⁷ There is a controversy about the non-equilibrium lesser and greater self-energies,^{25,26} which we do not address here. These quantities are discussed in detail in Ref. 26, where it is shown that all expressions satisfy basic Ward identities.
- ²⁸ L. Merker, S. Kirchner, E. Muñoz, and T. A. Costi, Phys. Rev. B **87**, 165132 (2013).
- ²⁹ A. A. Aligia, Phys. Rev. B **90**, 077101 (2014).
- ³⁰ L. Merker, S. Kirchner, E. Muñoz, and T. A. Costi, Phys. Rev. B **90**, 077102 (2014). There is a mistake in the ordinate axis in Fig. 2: it should be c'_B and not c_B .
- ³¹ D. C. Langreth, Phys. Rev. **150**, 516 (1966).
- ³² A. Yoshimori and A. Zawadowski, J. Phys. C **15**, 5241 (1982).
- ³³ A. C. Hewson, Phys. Rev. Lett. **70**, 4007 (1993).
- ³⁴ A. A. Aligia and L. A. Salguero, Phys. Rev. B **70**, 075307 (2004).
- ³⁵ A. A. Aligia, Phys. Rev. B **74**, 155125 (2006).
- ³⁶ P. S. Cornaglia and D. R. Grempel, Phys. Rev. B **71**, 075305 (2005).
- ³⁷ A. Kogan, S. Amasha, D. Goldhaber-Gordon, G. Granger, M. A. Kastner, and H. Shtrikman, Phys. Rev. Lett. **93**, 166602 (2004).
- ³⁸ D.M. Zumbühl, C.M. Marcus, M.P. Hanson, and A.C. Gosard, Phys. Rev. Lett. **93**, 256801 (2004).
- ³⁹ S. Amasha, I.J. Gelfand, M. A. Kastner, and A. Kogan, Phys. Rev. B **72** 045308 (2005).
- ⁴⁰ T-M. Liu, B. Hemingway, A. Kogan, S. Herbert, and M. Melloch, Phys. Rev. Lett. **103**, 026803 (2009).
- ⁴¹ G. D. Scott, D. Natelson, S. Kirchner, and E. Muñoz, Phys. Rev. B **87**, 241104(R) (2013).
- ⁴² T. A. Costi, Phys. Rev. B **64**, 241310(R) (2001).
- ⁴³ D.E. Logan and N.L. Dickens, J. Phys. Cond. Matt. **13**, 9713 (2001).
- ⁴⁴ A. Rosch, T. A. Costi, J. Paaske, and P. Wölfle, Phys. Rev. B **68**, 014430 (2003).
- ⁴⁵ T. Fujii and K. Ueda, J. Phys. Soc. Jpn. **74**, 127 (2005).
- ⁴⁶ A. Rosch, J. Paaske, J. Kroha, and P. Wölfle, Phys. Rev. Lett. **90**, 076804 (2003).
- ⁴⁷ A. C. Hewson, J. Bauer, and A. Oguri, J. Phys. Cond. Matt. **17**, 5413 (2005).
- ⁴⁸ C. J. Wright, M. R. Galpin, and D. E. Logan, Phys. Rev. B **84**, 115308 (2011).
- ⁴⁹ L. Tosi and A. A. Aligia, Phys. Status Solidi B **248**, 732-740 (2011).
- ⁵⁰ L. G. G. V. Dias da Silva, E. Vernek, K. Ingersent, N. Sandler, and S. E. Ulloa, Phys. Rev. B **87**, 205313 (2013).
- ⁵¹ P. Roura-Bas, L. Tosi, A. A. Aligia, and P. S. Cornaglia, Phys. Rev. B **86**, 165106 (2012).
- ⁵² Th. Pruschke and N. Grewe, Z. Phys. B **74**, 439 (1989).
- ⁵³ D. E. Logan, M. P. Eastwood, and M. A. Tusch, J. Phys. Condens. Matter **10**, 2673 (1998).
- ⁵⁴ A. A. Aligia, P. Roura-Bas, and S. Florens, Phys. Rev. B **92**, 035404 (2015).
- ⁵⁵ This can be checked using for example perturbation theory in the Coulomb repulsion U up to second order,^{56,57} which in the symmetric case $E_d = -U/2$ is accurate for $U/\Delta \leq 2\pi$.⁵⁸
- ⁵⁶ K. Yosida and K. Yamada, Prog. Theor. Phys. Suppl. **46**, 244 (1970); Prog. Theor. Phys. **53**, 1286 (1975); K. Yamada, *ibid* **53**, 970 (1975).
- ⁵⁷ B. Horvatić and V. Zlatić, Phys. Rev. B **30**, 6717 (1984); B. Horvatić, D. Šokčević, and V. Zlatić, *ibid* **36**, 675 (1987).
- ⁵⁸ R. N. Silver, J. E. Gubernatis, D. S. Sivia, and M. Jarrell, Phys. Rev. Lett. **65**, 496 (1990).
- ⁵⁹ J.E. Moore and X-G Wen, Phys. Rev. Lett. **85**, 1722 (2000).
- ⁶⁰ While the explicit results of Ref. 54 were obtained using the non-crossing approximation, the result that for highly asymmetric devices in the Kondo regime, the differential conductance $G = dI/dV_b$ near zero applied bias voltage V_b reproduces the spectral density of the Kondo peak is based on general physical arguments and known properties of the Kondo resonance and does not depend on the approximation.
- ⁶¹ Y. Meir and N. S. Wingreen, Phys. Rev. Lett. **68**, 2512 (1992); A-P. Jauho, N.S. Wingreen, and Y. Meir, Phys. Rev. B **50**, 5528 (1994).
- ⁶² S. R. White, Phys. Rev. Lett. **69**, 2863 (1992); U. Schollwöck, Ann. Phys. (NY) **326**, 96 (2011); K. Hallberg, Adv. Phys. **55**, 477 (2006).
- ⁶³ S. Nishimoto and E. Jeckelmann, J. Phys.: Condens. Matter **16**, 613 (2004).
- ⁶⁴ A. Weichselbaum, F. Verstraete, U. Schollwöck, J. I. Cirac, and Jan von Delft, Phys. Rev. B **80**, 165117 (2009).
- ⁶⁵ L. G. V. Dias da Silva, F. Heidrich-Meisner, A. E. Feiguin, C. A. Büsler, G. B. Martins, E. V. Anda, and E. Dagotto, Phys. Rev. B **78**, 195317 (2008).
- ⁶⁶ H. R. Krishna-murthy, J. W. Wilkins, and K. G. Wilson, Phys. Rev. B **21**, 1003 (1980); *ibid* **21**, 1044 (1980).
- ⁶⁷ R. Bulla, T. A. Costi, and Th. Pruschke, Rev. of Mod. Phys. **80**, 395 (2008).
- ⁶⁸ V. L. Campo and L. N. Oliveira, Phys. Rev. B **72**, 104432 (2005).
- ⁶⁹ L. Merker, A. Weichselbaum, T. A. Costi, Phys. Rev. B **86**, 075153 (2012).
- ⁷⁰ A. C. Hewson, A. Oguri, and D. Meyer, Eur. Phys. J. B **40**, 177 (2004).
- ⁷¹ P. B. Wiegmann and A. M. Tsvetick, J. Phys. C: Solid State Phys., **16** 2281 (1983).
- ⁷² A. A. Aligia, C. A. Balseiro, and C. R. Proetto, Phys. Rev. B **33** 6476 (1986).
- ⁷³ I. J. Hamad, P. Roura-Bas, A. A. Aligia, and E. V. Anda, arXiv:1506.06847.
- ⁷⁴ V. Zlatić and B. Horvatić, Phys. Rev. B **28**, 6904 (1983).
- ⁷⁵ A. Martín-Rodero, M. Baldo, F. Flores, and R. Pucci, Solid State Commun. **44**, 911 (1982).
- ⁷⁶ A. Martín-Rodero, E. Louis, F. Flores, and C. Tejedor, Physical Review B **33**, 1814 (1986).
- ⁷⁷ A. Levy-Yeyati, A. Martín-Rodero, and F. Flores, Phys. Rev. Lett. **71**, 2991 (1993).
- ⁷⁸ H. Kajuter and G. Kotliar, Phys. Rev. Lett. **77**, 131(1996).
- ⁷⁹ A.A. Aligia and C.R. Proetto, Phys. Rev. B **65**, 165305 (2002).
- ⁸⁰ I. Maruyama, N. Shibata, and K. Ueda, J. Phys. Soc. Jpn. **73**, 3239 (2004).

- ⁸¹ A. Camjayi and L. Arrachea, *J. Phys. Condens. Matter* **26**, 035602 (2014).
- ⁸² J. Könemann, B. Kubala, J. König, and R. J. Haug, *Phys. Rev. B* **73**, 033313 (2006).
- ⁸³ J. Park, Ph. D Thesis, University of California (2003).
- ⁸⁴ L. Vaugier, A.A. Aligia and A.M. Lobos, *Phys. Rev. B* **76**, 165112 (2007).
- ⁸⁵ F. D. M. Haldane, *Phys. Rev. Lett.* **90**, 416 (1978).